A NOTE ON RECENT EXPERIMENTS WITH ROSSBY WAVES ON EASTWARD JETS

L.M. POLVANI* AND JIHAD TOUMA†

Abstract. Sommeria, Meyers and Swinney (1989) have recently conducted experiments with Rossby waves on eastward jets in a rotating annular tank. Exploiting the simplicity of the observed potential vorticty field, we construct here a simple model that captures the basic dynamics of these waves, and discuss the occurance of chaotic mixing this flow.

1. Introduction. In a series of recent experiments Sommeria, Meyers and Swinney (1989, hereafter SMS) have studied the behavior of eastward jets in rotating flows. A layer of constant density fluid is spun up in a rotating annular tank whose bottom is conical in shape (to simulate the β-effect). An array of sinks and sources at the bottom of the tank are then activated to generate an azimuthal jet in the middle of the annular region. The instability of the initial velocity profile generates large amplitude waves that are observed propagating along the jet. Die injected in the flow is observed to mix rapidly on either side of the jet, but little exchange takes place across the jet.

Motivated by the surprisingly simple structure of the potential vorticity field observed in the experiments, we construct a simple model that captures the essential dynamics of Rossby waves on eastward jets in the annular geometry. The simplicity of the model allows us to solve the dynamical equations for the flow and derive both a solution for the jet satisfying the appropriate boundary conditions (§2), and the dispersion relation for Rossby waves on the jet (§3). From these linear results, we discuss the chaotic mixing induced by the waves and suggest nonlinear extensions of this model (§4).

2. A simple model for the jet. The starting point of our analysis is the observation that, in the experiments of SMS, the potential vorticity q assumes a remarkably simple configuration once the jet and the waves are fully developed. The gradients of potential vorticity are found to be concentrated in a narrow band near the jet, and q is very nearly homogeneous on either side of the jet (cf. Fig. 1c of SMS). This suggests that the essential physics of this problem can be captured by the dynamics of a *single interface* of potential vorticity.

In polar coordinates (r, ϑ), we therefore consider the following distribution of potential vorticity (illustrated in Fig. 1):

$$q = \begin{cases} q_1 & \text{if} \quad r_1 < r < r_{jet}(\vartheta) \\ q_2 & \text{if} \quad r_{jet}(\vartheta) < r < r_2 \end{cases} \tag{1}$$

where q_1 and q_2 are constants, r_1 and r_2 are the inner and outer boundaries of the

* Department of Applied Physics, Columbia University, New York, NY 10027,
† Department of Mathematics, Massachusetts Institute of Technology, Cambridge MA 02139

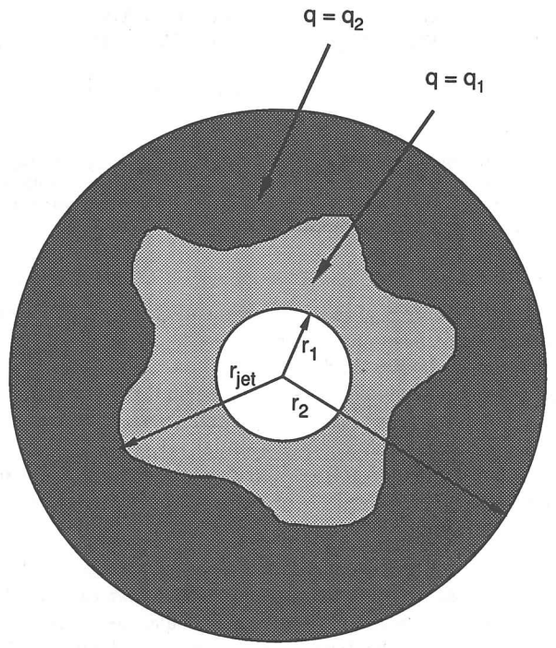

Figure 1: A sketch of the distribution of potential vorticity q in our simple model for the eastward jet. The value of q is taken to be constant and uniform inside and outside the jet. Contrast this figure with Fig. 1c of SMS.

annulus, and $r_{jet}(\vartheta)$ defines the position of the potential vorticity interface, i.e. the jet. For later reference, we designate by D_i ($i = 1,\ 2$) the region where $q = q_i$. Notice that this is only the simplest model, and complexity can be added by considering several nested interfaces delimiting undulating annular regions of uniform potential vorticity.

As described in SMS, the flow is quasigeostrophic and essentially inviscid, and the potential vorticity is very nearly conserved. Except near the side walls and the bottom of the tank where we expect thin boundary layers to exist (the Ekman number is typically of the order of 10^{-6} in these experiments), a streamfunction ψ can be used to describe the two-dimensional flow. The dynamics is governed by the material conservation of potential vorticity:

$$\frac{D}{Dt}q = [\partial_t + J(\psi, \cdot)]q = 0 \tag{2}$$

where q is given by:

$$q = \nabla^2\psi + \beta r. \tag{3}$$

There are two components to the potential vorticity. The first is due to the vorticity of the flow relative to the rotating tank. The second is due to the vortex stretching

caused by the sloping bottom, the familiar β-effect. Here β is defined by:

$$\beta = \frac{2\omega s}{h_0} \tag{4}$$

where ω is the angular velocity of the rotating tank, s is the slope of the bottom and h_0 is the average height of the fluid column. The radial and azimuthal velocities (u and v respectively) are obtained from the streamfunction via:

$$u = -\frac{1}{r}\frac{\partial\psi}{\partial\vartheta} \qquad \text{and} \qquad v = \frac{\partial\psi}{\partial r} \tag{5}$$

The first task is to determine the structure of the jet in the absence of waves. This means solving (2) for the streamfunction ψ with q given by (1) with $r_{jet}(\vartheta) = r_0$. Since for the undisturbed jet ψ is only a function of radius (2) is immediately satisfied, and we are left with the inversion of (3). This is easily accomplished and yields:

$$\psi_i = -\frac{1}{9}\beta r^3 + \frac{1}{4}q_i r^2 + c_i \log r \qquad \text{in} \quad D_i, \tag{6}$$

where $i = 1,\ 2$ for the inner and outer regions, respectively. The constants c_i are chosen to satisfy the no-slip boundary condition at $r = r_i$, and are found to be:

$$c_i = \left[\frac{1}{3}\beta r_i - \frac{1}{2}q_i\right] r_i^2. \tag{7}$$

Finally we must require that the velocity be continuous at $r = r_0$. This condition yields a constraint between q_1, q_2 and r_0. Thus, given q_1 and q_2 the position of the jet is uniquely determined by a dynamical equilibrium, and is given by:

$$r_0 = \left[\frac{2(c_1 - c_2)}{q_1 - q_2}\right]^{1/2} \tag{8}$$

As an example, for the typical values $r_1 = 10.8$cm, $r_2 = 43.2$cm, $q_1 = -2\text{s}^{-1}$, $q_2 = -8\text{s}^{-1}$, $\omega = 18.8\text{s}^{-1}$ and $h_0 = 18.7$cm (giving $\beta = -0.2\text{cm}^{-1}\text{s}^{-1}$), constraint (8) gives $r_0 = 26$cm, which puts the jet essentially in the middle of the annulus (cf. Fig. 1c of SMS).

For these same values the velocity profile for the jet is shown in Fig. 2. The velocity maximum has a value around 20cm s^{-1}. It should be pointed out that this profile is the result of the cancellation between two large contributions, an eastward velocity due to β – the first term in (6) – and a strong westward flow due to the negative values q. Hence there is a strong sensitivity of the velocity profile to the values of the parameters.

3. Rossby waves on the jet. We next consider the question of perturbations on this jet profile. Since the q profile is monotonic with radius, we expect that all perturbations will be stable. In the usual fashion, we consider perturbations that merely displace the potential vorticity interface. Our analysis closely follows the classic one of Lord Kelvin for perturbations of the Rankine vortex (Lamb, 1932). Let

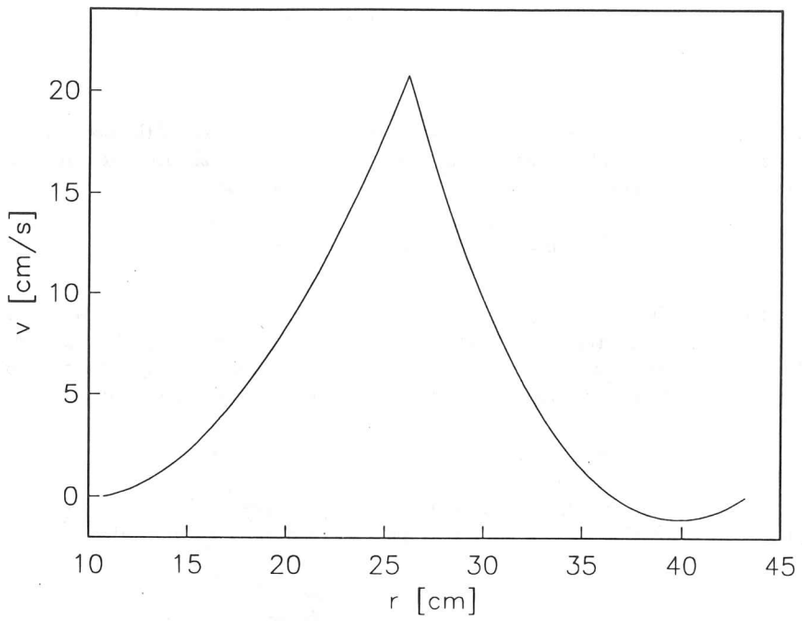

Figure 2: A typical velocity profile for the eastward jet from our simple model. The parameter values here are: $r_1 = 10.8\text{cm}$, $r_2 = 43.2\text{cm}$, $q_1 = -2\text{s}^{-1}$, $q_2 = -8\text{s}^{-1}$, $\omega = 18.8\text{s}^{-1}$.

φ_i be the streamfunction associated with the perturbation in D_i. Since φ_i satisfies Laplace's equation, we can immediately write:

$$\varphi_i = \varepsilon \left(A_i r^m + B_i r^{-m}\right) \cos(m\vartheta - \Omega t) \tag{9}$$

The position of the perturbed boundary is given by:

$$r = r_0 + \eta(\vartheta, t) = r_0 \left[1 + \varepsilon \cos(m\vartheta - \Omega t)\right] \tag{10}$$

where ε is a nondimensional number representing the amplitude of the perturbation. A number of appropriate boundary conditions need to be applied. These are (in linearized form): continuity of radial velocity at the potential vorticity interface,

$$\partial_\vartheta \varphi_1 = \partial_\vartheta \varphi_2 \quad \text{at} \quad r = r_0 \,, \tag{11}$$

continuity of tangential velocity at the potential vorticity interface,

$$\partial_r \varphi_1 + \eta \partial_r^2 \psi_1 = \partial_r \varphi_2 + \eta \partial_r^2 \psi_2 \quad \text{at} \quad r = r_0 \,, \tag{12}$$

no radial velocity at the inner boundary of the annulus,

$$\partial_\vartheta \varphi_1 = 0 \quad \text{at} \quad r = r_1 \,, \tag{13}$$

no radial velocity at the outer boundary of the annulus,

$$\partial_\vartheta \varphi_2 = 0 \quad \text{at} \quad r = r_2 \,, \tag{14}$$

and a kinematic condition insuring that the radial velocity of the fluid at the interface is identical to that of the interface itself:

$$\frac{D}{Dt}\eta = \left[\partial_t + \frac{1}{r}(\partial_r \psi)\right] \eta = -\frac{1}{r}\partial_\vartheta \varphi \quad \text{at} \quad r = r_0 \,. \tag{15}$$

It is not possible to impose that the azimuthal velocity associated with the perturbation vanish at the walls of the tank, and thus the no-slip boundary condition is not satisfied by the perturbation velocity fields. In practice, however, the azimuthal velocities induced by the perturbation are extremely small at the walls, especially for the higher wavenumbers (see below).

Substitution of (9) and (10) into the above constraints, yields, after some simple algebra, the dispersion relation for these waves:

$$\frac{\Omega}{m} = \frac{v_0}{r_0} - \frac{1}{2m} \Delta q \, \mathcal{F}_m(r_1, r_2, r_0) \tag{16}$$

where $v_0 \equiv -(1/3)\beta r_0^2 + (1/2) q_1 r_0 + c_1/r_0$ is the undisturbed azimuthal velocity on the vorticity interface, $\Delta q = q_1 - q_2$ is the jump in potential vorticity across the interface, and

$$\mathcal{F}_m(r_1, r_2, r_0) = \frac{(r_2^{2m} - r_0^{2m})(r_0^{2m} - r_1^{2m})}{r_0^{2m}(r_2^{2m} - r_1^{2m})} \tag{17}$$

is a nondimensional function related to the annular geometry of the tank.

Note first that the β-effect enters only through v_0, and thus the presence of a conical bottom leads to a simple Doppler shift in the frequency of these waves. Also, it is easily seen that $\mathcal{F} \to 1$ in the limit $r_1 \to 0, r_2 \to \infty$, so that (16) reduces to the

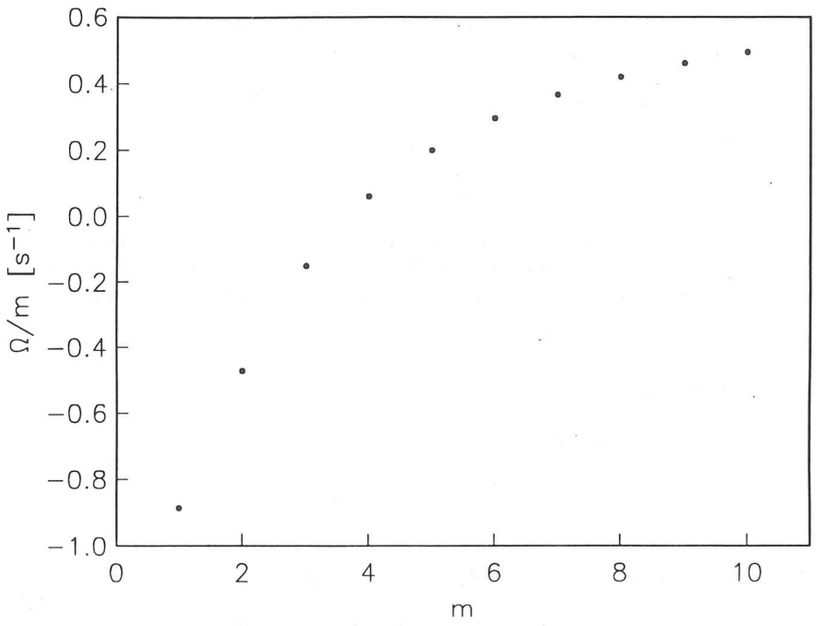

Figure 3: The angular velocity for Rossby waves on the jet as a function of wavenumber, for the parameter values that give the jet shown in Fig 2.

familiar result for waves on the Rankine vortex (Lamb, 1932). Finally, notice that, since $\mathcal{F} > 0$, the phase speed in a frame that rotates with angular velocity v_0/r_0 is always negative (for $\Delta q > 0$); this is a clear signature that these waves are indeed Rossby waves, since their phase propagation is always westward for an observer that is advected by the jet.

For the values of potential vorticity used to obtain the jet shown in Fig. 2, the dispersion relation is shown graphically in Fig. 3. Notice that the low wavenumbers have negative values of Ω/m; this has profound consequences on the question of chaotic mixing, as will be explained in the next section.

To complete the linear analysis of these Rossby waves, we find that the amplitudes of the perturbation streamfunction are given by:

$$(A_i, B_i) = -\frac{1}{2m}\,\Delta q\,(a_i, b_i) \tag{18}$$

with:

$$a_i = \frac{r_i^{2m} - r_0^{2m}}{r_2^{2m} - r_1^{2m}} \qquad \text{and} \qquad b_i = -\,r_i^{2m}\,a_i \tag{19}$$

From these expressions, one can compute the value of the azimuthal velocity at the annular boundary due to the Rossby waves on the jet. As already mentioned,

these velocities are extremely small for parameter values relevant to the experiments of SMS and, moreover, they decay exponentially with m. For the parameter values of Fig. 2, the values v_1 and v_2 of the azimuthal velocities induced by a single wave at $r = r_1$ and r_2 respectively are given in Table 1.

Table 1. The azimuthal velocities v_1 and v_2 induced by a Rossby wave of amplitude $\varepsilon = 0.1$ at the inner and outer annular walls respectively. The values decrease exponentially with m.

m	v_1 [cms^{-1}]	v_2 [cms^{-1}]
2	$1.243\ 10^{-3}$	$-3.281\ 10^{-2}$
3	$7.349\ 10^{-6}$	$-2.262\ 10^{-3}$
4	$4.269\ 10^{-8}$	$-1.472\ 10^{-4}$
5	$2.472\ 10^{-10}$	$-9.381\ 10^{-6}$
6	$1.431\ 10^{-12}$	$-5.934\ 10^{-7}$
7	$8.282\ 10^{-15}$	$-3.743\ 10^{-8}$
8	$4.792\ 10^{-17}$	$-2.359\ 10^{-9}$
9	$2.773\ 10^{-19}$	$-1.486\ 10^{-10}$
10	$1.605\ 10^{-21}$	$-9.364\ 10^{-12}$

4. Chaotic mixing. In the experiments of SMS, one usually observes a single dominant wave on which several other waves of smaller amplitude are superimposed. It is natural then to change to a frame of reference that rotates with the angular velocity of the dominant wave. As is well known, it is the analysis of the streamfunction in that frame that yields insight into the integrability of passive particle trajectories. In the presence of a single wave, the corotating streamfunction ψ^c is defined by:

$$\psi_i^c(r, \vartheta') = \psi_i(r) + \varepsilon(A_i r^m + B_i r^{-m})\cos(\vartheta') - \frac{1}{2}\left(\frac{\Omega}{m}\right) r^2 \tag{20}$$

where ψ_i is given in (6) and $\vartheta' \equiv \vartheta - (\Omega/m)t$ is the azimuthal angle in the frame rotating with the angular velocity of the wave. Since the time dependence is eliminated from the streamfunction by moving into the corotating frame, it is obvious that no chaotic mixing can occur if only a single wave is present. The addition of a second wave is necessary to produce a time modulation. This is not, however a sufficient condition for chaotic mixing. It is also necessary that the corotating streamfunction (20) possess saddle stagnation points. The presence of these is determined by solving:

$$\partial_r \psi_i^c(r_c, \vartheta_c') = 0 \qquad \text{and} \qquad \partial_{\vartheta'} \psi_i^c(r_c, \vartheta_c') = 0\ . \tag{21}$$

for r_c and ϑ_c'. To lowest order in ε these give $\vartheta_c = n\pi/m,\ n = 0, 1, \ldots, (2m-1)$ and:

$$v_i(r_c) = \partial_r \psi_i(r_c) = \left(\frac{\Omega}{m}\right) r_c \tag{22}$$

i.e. the stagnation points are the locations where the velocity of the undisturbed jet equals the velocity of the wave. Since the jet is eastward (i.e. $v_i > 0$), (22) has no solution when $(\Omega/m) < 0$. This typically occurs for the low wavenumbers ($m < 4$ for the parameter values used in Fig. 2). We expect that when no resonances occur

in the corotating streamfunctions associated with the dominant wave chaotic mixing (usually occurring as the smaller amplitude waves perturb the dominant one) should be highly suppressed.

For $(\Omega/m) > 0$ there are two values of r_c that solve (22), one on each side of the jet, yielding a streamfunction pattern sketched in Fig. 4. A single wave with sufficiently large azimuthal wavenumber m will generate $2m$ stagnation points on each side of the jet; m of these are saddle points and m are the centers of as many "ghost" vortices. Typically, as m increases the stagnation points approach the edge of the jet, while at low m they are closer to the annular walls. For the parameter values that give the jet in Fig. 3, the location of the stagnation points obtained by solving (22) is given in Table 2. In the presence of a second wave, the pattern in Fig. 4 is perturbed and becomes time dependent. Chaotic mixing is then expected to occur on either side of the jet, but, as long as the waves don't break particles cannot cross the potential vorticity boundary.

Table 2. The radial positions r_1 and r_2 of the inner and outer stagnation points as a function of wavenumber for the parameter values on Fig. 3. The undisturbed jet is located at $r_0 = 26.2$ cm.

m	r_1 [cm]	r_2 [cm]
4	12.9	34.4
5	16.1	31.6
6	17.8	30.3
7	19.1	29.5
8	20.1	29.5
9	20.7	28.6
10	21.3	28.3

One could at his point use a linear superposition of a small number of linear waves and advect passive tracer particles with the velocity field induced by the waves. One such study has been carried out by Behringer *et al.* (1991) using linear waves derived phenomenologically from the experimental data; the presence of large zones of chaotic mixing in this flow has been confirmed. The next step ought to take into account the nonlinear dynamical interaction between the waves.

Such a nonlinear study is beyond the scope of this brief note. We suggest that extending the methods of Contour Dynamics and Countour Surgery (Dritschel 1989) to the annular geometry of this problem offers an attractive possibility. Since these methods are Lagrangian, they are ideally suited to study chaotic mixing, as well as the nonlinear dynamics of the waves.

Acknowledgements. LMP wishes to thank Prof. Harry Swinney for bringing this problem to his attention, Dr. Steve Meyers for useful discussions on the experiments, and Prof. Harvey Greenspan of MIT for an illuminating conversation on boundary layers in rotating tanks. This work was supported, in part, by the Atmospheric Science Division of the NSF, under grant 8911459-ATM.

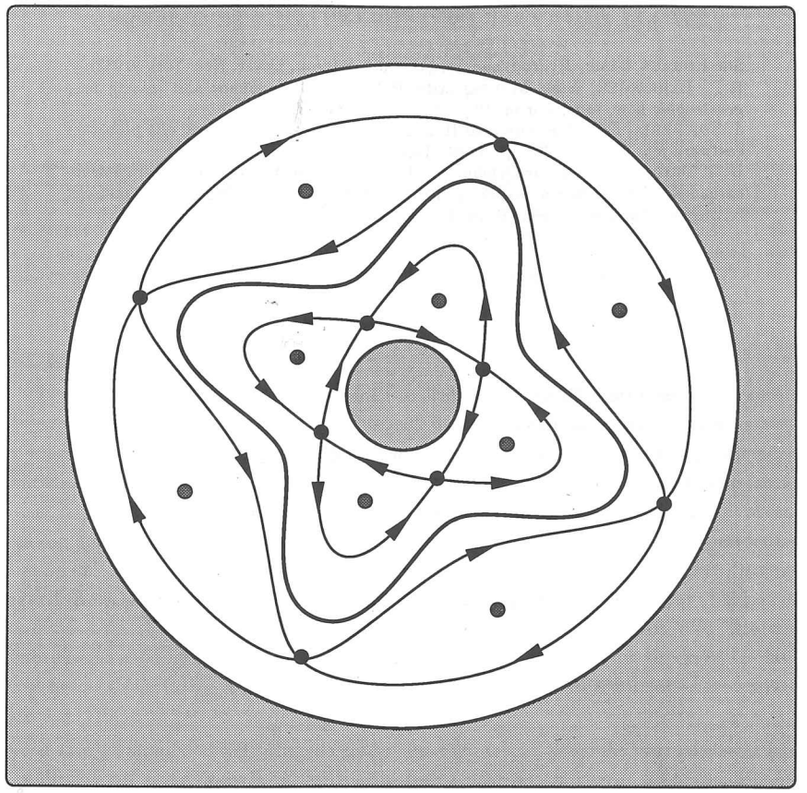

Figure 4: A sketch of the geometry of the corotating streamfunction associated with an $m = 4$ wave on the potential vorticity interface. The grey dots are the centers of the "ghost" vortices. The black dots are the saddle points. The solid lines are the separatrices, while the thick line shows the position of the potential vorticity interface.

REFERENCES

SIR HORACE LAMB, *Hydrodynamics*, §158, 6th Edition, Dover, New York (1932).

R.P. BEHRINGER, S.D. MEYERS AND H.L. SWINNEY, *Chaos and mixing in a geostrophic flow*, to appear in Phys. Fluids A, 3 (1991).

J. SOMMERIA, S.D. MEYERS AND H.L. SWINNEY, *Laboratory model of a planetary eastward jet*, Nature, 337, pp. 58-61 (1989).

D.G. DRITSCHEL, *Contour Dynamics and Contour Surgery: numerical algorithms for extended, high-resolution modelling of vortex dynamics in two-dimensional, inviscid, incompressible flows*, Comp. Phys. Rep., 10 (3), pp. 77-146 (1989).